Journal Name

ARTICLE TYPE

Cite this: DOI: 10.1039/xxxxxxxxxx

# Experimental study on the thermal desorption of formamide

Riccardo Giovanni Urso *[ab], Carlotta Scirè [b], Giuseppe Antonio Baratta [b], John Robert Brucato [c], Giuseppe Compagnini [a], Zuzana Kaňuchová [db], Maria Elisabetta Palumbo [b] and Giovanni Strazzulla [b]

Received Date
Accepted Date

DOI: 10.1039/xxxxxxxxxx

www.rsc.org/journalname

Laboratory experiments have shown that the energetic processing, i.e. ion bombardment and UV photolysis, of interstellar grain mantles and cometary surfaces is efficient in the production of formamide. To explain its presence in the gas-phase in these astrophysical environments, a desorption mechanism has to be taken into account. In this work we show experimental results on the thermal desorption of formamide when deposited at 17 K as pure and in mixture with water or carbon monoxide. In these samples, we observed formamide desorption at 220 K. Moreover, we discuss about its synthesis in a mixture containing molecular nitrogen, methane and water ($N_2$:$CH_4$:$H_2O$) deposited at 17 K and bombarded with 200 keV $H^+$. Heating the sample, we observed that the newly formed formamide remains trapped in the refractory residue produced after the ion bombardment up to 296 K. To analyse the samples we used Fourier transform-infrared spectroscopy (FT-IR) that allowed us to study the infrared spectra between the deposition and the complete desorption of formamide. Here we discuss the experimental results in view of their astrophysical relevance.

## 1 Introduction

Formamide, also known as methanimide ($NH_2CHO$), is a molecule that belongs to the amides family and includes a peptide bond. It has been shown that it can act as a precursor in the synthesis of many interesting compounds by a biological point of view, as amino and nucleic acids [1–4], making it one of the possible players in pre-biotic chemistry. Formamide has been detected in several astrophysical environments. In particular, it has been observed in the gas phase in some star forming regions in space [5–7]. In these regions gas and dust start to accumulate toward the centre of a cold cloud, so that a star eventually forms. About 200 molecules* have been detected in the gas phase toward these regions by means of ground based radio telescopes. Using both ground based or space infrared telescopes a few molecules have been detected also in the solid phase, where they are found on the surface of silicates or carbonaceous dust grains, forming the so called *icy grain mantles*.

During the star formation process, the chemical complexity of icy grain mantles increases because of their interaction with other gas-phase species (mainly atomic hydrogen), UV-photons and cosmic rays. In particular, cosmic rays are highly energetic charged particles that bombard the icy mantles and release a fraction of their energy to the target, modifying their chemical composition [8,9]. During the further stages of stellar formation, a protoplanetary disk forms and temperature increases in the region closer to the star. Because of the heating, molecules that were frozen on the icy grain mantles sublimate in the gas-phase, where

[a] *Dipartimento di Scienze Chimiche, Università degli Studi di Catania, Viale Andrea Doria 6, 95125 Catania, Italy. Tel: +390957332201; e-mail: rurso@oact.inaf.it*
[b] *INAF-Osservatorio Astrofisico di Catania, via Santa Sofia 78, 95123 Catania, Italy*
[c] *INAF-Osservatorio Astrofisico di Arcetri, Largo Enrico Fermi 5, 50125 Firenze, Italy.*
[d] *Astronomical Institute of Slovak Academy of Sciences, 05960 Tatranská Lomnica, Slovakia*

* https://www.astro.uni-koeln.de/cdms/molecules

they can further react and form new and more complex species. Only dust grains that are in the outer shell of the protoplanetary disk can preserve at least partially their icy mantles. Moreover, they can also be enriched of newly formed species coming from the gas-phase. Thanks to the comparison between the spectra acquired by means of infrared telescopes toward several sources in space and the data coming from laboratory experiments in which icy grain mantles analogues are synthesized, it has been possible to determine their physical structure[10,11] and chemical composition. In particular, it has been possible to detect water and carbon monoxide as the main constituents of icy mantles, together with carbon dioxide, methane, methanol and ammonia[12–16]. Other species, such as formaldehyde, sulfur dioxide and carbonyl sulphide have been likely detected[12,17,18]. Furthermore, Schutte *et al.*[19] and Raunier *et al.*[20] reported a tentative detection of solid formamide in the line of sight of young stellar objects observed with the Infrared Space Observatory-Short Wavelenght Spectrometer (ISO-SWS). It is generally accepted that dust grains coagulate into larger objects named planetesimals that are the building blocks of future planets, comets and asteroids[21]. In this scenario, it is particularly interesting the detection of formamide in the coma of comets C/1995 O1 Hale-Bopp[22], C/2012 F6 Lemmon and C/2013 R1 Lovejoy[23].

To date, there is an open debate about formamide synthesis in space, in particular if it occurs directly in the gas phase in star forming regions, where it has been firmly detected, or in the solid phase, i.e., on the icy mantles of dust grains or on the surface of comets. Recent thermochemical and kinetic computations have shown that formamide can be produced at low temperature in the gas-phase by the reaction of formaldehyde ($H_2CO$) with $NH_2$[24,25]. On the other hand, laboratory experiments have shown that formamide is produced after the energetic processing, i.e., ion and electron bombardment and UV-photolysis that simulate the effects of cosmic rays and UV-photons in space, of mixtures that are thought to be representative of icy mantles and cometary surfaces[26–29].

Kaňuchová *et al.*[29] have shown that the irradiation with protons or helium ions of different solid mixtures contanining water, methane, ammonia or nitrogen at low temperatures drives the synthesis of formamide together with isocyanic acid (HNCO). They compared the $HNCO/NH_2CHO$ molecular number ratio obtained from laboratory data with that obtained from observations. Their results showed that in most cases the ratio obtained in laboratory experiments is lower than the ratio observed in star forming regions, suggesting that the abundance of formamide in star forming regions can be ascribed to energetic processing of icy mantles while other processes, such as gas-phase and grain surface reactions, have to be taken into account to explain the observed abundances of isocyanic acid. Also, concerning comets, they showed that energetic processing can explain the observed amount of formamide, while HNCO cannot be produced in significant amount.

Once it has been proved that energetic processing is efficient in the formation of $NH_2CHO$, it is important to understand how this molecule is injected into the gas phase. Dawley *et al.*[30] have reported on the thermal desorption of pure formamide. In their experiments, they have deposited the amide on porus silicon oxide nanoparticles at 70 K and they have followed by means of infrared spectroscopy the sample warm up until its complete desorption. They have observed that formamide crystallize at about 165 K and it starts to desorb from the $SiO_2$ substrate at 210 K. The complete desorption requires about 380 K. They have also investigated the desorption of a $H_2O$:$NH_2CHO$=2:1 mixture. In this experiment water sublimates at about 160 K, leaving formamide on the substrate that then follows the same behaviour shown when deposited in pure form.

To the best of our knowledge, there is a lack of data about the thermal desorption of formamide when in mixture with other astrophysical relevant molecules. In this paper we report the data we collected during experiments about the sublimation of solid films containing pure formamide and formamide in mixture with water and carbon monoxide, the most abundant solid phase molecules in space, in order to simulate its desorption from the icy grain mantles and cometary surfaces. We also show experimental results about the ion bombardment with 200 keV $H^+$of a mixture containing nitrogen, methane and water to discuss about the desorption of formamide when synthesised after energetic processing at low temperature. The experiments allowed us to determine the crystallization and desorption temperature of formamide when pure and in mixtures and to apply these results to an astrophysical context.

## 2 Experimental methods

The experiments here shown have been performed in the Laboratory for Experimental Astrophysics at INAF-Osservatorio Astrofisico di Catania (Italy). We carried out two different sets of experiments, one to investigate the desorption temperature of formamide when pure and in mixture with water and carbon monoxide, and one to study its desorption when synthesised after irradiation of the sample with energetic ions (200 keV $H^+$). All the experiments have been performed in an ultra high vacuum (UHV) chamber ($P \leq 10^{-9}$ mbar) shown in Fig.1. Inside the UHV chamber a KBr substrate is placed in thermal contact with the final tail of a closed-cycle helium Cryocooler (CTI) which temperature can be varied between 17 and 300 K. In the first set of experiments, to avoid any interaction between gases before depositon, we introduced the species in two separate chambers at room temperature and $P<10^{-7}$ mbar. A chamber was dedicated to both water or CO, with a direct inlet in the UHV chamber (Inlet A in Fig.1), while in a second chamber we introduced formamide only, that

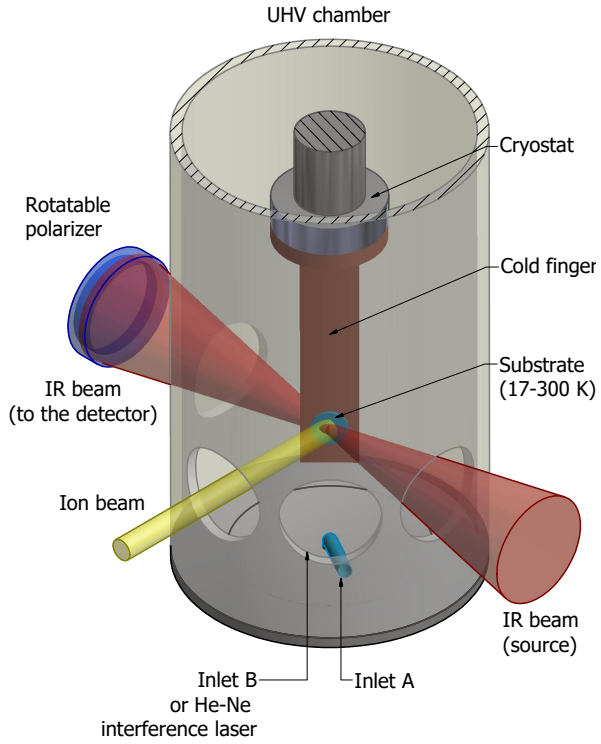


**Fig. 1** Schematic view of the UHV chamber and the geometry used to irradiate the sample and to acquire infrared spectra.

was then admitted in the UHV chamber by an inlet mounted on its lateral wall (Inlet B in Fig.1) simultaneously with water or CO. This set-up allowed us to obtain pure $NH_2CHO$, $NH_2CHO$:$H_2O$ and $NH_2CHO$:CO mixtures. In the second set of experiments, a $N_2$:$CH_4$:$H_2O$ mixture has been prepared in a vacuum chamber ($P<10^{-7}$ mbar) and introduced in the UHV chamber by the Inlet A in Fig.1. Once inside the UHV chamber, molecular species to be investigated condense on the cold substrate forming a solid film.

The $N_2$:$CH_4$:$H_2O$ film thickness has been measured during the deposition following the procedure described in Fulvio *et al.*[33] and Urso *et al.*[34]. An He-Ne laser beam ($\lambda$ = 543.5 nm) is directed toward the sample and reflected at near normal incidence (2.9°) both by the vacuum-sample and sample-substrate interfaces. The reflected beam is detected by an external silicon diode detector. There is a difference in the optical path between the reflected components of the laser beam that varies with the thickness of the film, so that an interference curve is produced. It is possible to follow the accretion of the film by looking at the interference curve (intensity vs. time) of the reflected laser beam[34].

After deposition, the $N_2$:$CH_4$:$H_2O$=1:1:1 mixture was then irradiated with 200 keV $H^+$. The vacuum chamber is connected to a 200 kV ion implanter by Danfysik. The ion beam is electrostatically swept to ensure a uniform coverage on the target. In order to prevent a macroscopic heating of the sample we used an ion current density between 100 nA $cm^{-2}$ and a few $\mu$A $cm^{-2}$. The ion fluence (ions $cm^{-2}$) was measured by integrating the ion current monitored during irradiation. We calculated the energy deposited by incoming ions to the sample (dose) by multiplying the fluence and stopping power (i.e., the amount of energy deposited per unit path length; eV $cm^2$/molecule) given by SRIM code[31]. The dose is given in eV/16u, which is a convenient way to characterize chemical changes and also to allow a comparison with other irradiation experiments[32].

All the samples were analyzed using infrared spectroscopy. Infrared transmission spectra were acquired at oblique incidence (45°) by a Fourier transform infrared (FTIR) spectrometer (Bruker Vertex 70) with a resolution of 1 $cm^{-1}$ and sampling of 0.25 $cm^{-1}$. A rotatable polarizer placed along the path of the IR beam allows us to take spectra both with the electric vector parallel (*p-polarized*) and perpendicular (*s-polarized*) to the plane of incidence of the infrared beam. In this work we will show the spectra acquired in *p-polarization* because of a better signal-to-noise ratio. We performed several steps of warm up for each sample to determine the formamide desorption temperature. We acquired transmission infrared spectra of the samples as deposited and after each step of irradiation and warm up. Also, during the experiments we set the spectrometer in a monitoring configuration that allows to check the infrared spectrum of the sample by means of fast and continuous acquisitions. In this way it was possible to stop the warm up and acquire a spectrum if some change would appear. See Palumbo *et al.*[35] and Kaňuchová *et al.*[29] for more details about the experimental procedure.

## 3 Results

Three experiments have been carried out by depositing pure $NH_2CHO$ and mixtures $NH_2CHO$:$H_2O$=1:14 and $NH_2CHO$:CO=1:40 at 17 K and warming up the samples until their complete desorption from the substrate. The mixtures we deposited contain formamide in the highest dilution we have been able to obtain in our experimental conditions, in order to be as close as possible to astrophysical context where this molecule is expected to be highly diluted. Furthermore, we performed an irradiation experiment in which we deposited a $N_2$:$CH_4$:$H_2O$=1:1:1 mixture at 17 K that has been bombarded with 200 keV $H^+$ to simulate the effects of cosmic-rays on icy grain mantles and comets. After irradiation we warmed up the sample to study the desorption of the synthesized formamide.

In Fig.2 we show the IR spectra of pure formamide, formamide in mixture with water and formamide in mixture with carbon monoxide at 17 K (left panel) and at 170 K (right panel). After the deposition, we started the desorption experiment in a step-by-step procedure: we increased the cryostat temperature up to a certain value, then we waited for the temperature stabilization before spectra acquisitions. For clarity, we do not show the region

without vibrational bands attributed to formamide, i.e. between 2700 and 1840 $cm^{-1}$.

### 3.1 Pure formamide

In Fig.2 A we show the IR spectrum of pure formamide deposited at 17 K. All the known vibrational features are labelled. Spectra have been acquired at 17, 30, 35, 140, 160 and 170 K. We chose these temperatures because formamide is stable until about 160 K, when a structural change starts to take place, as reported by Dawley *et al.*[30]. In our experiments no changes appeared in the infrared spectra until the sample reached 170 K. At this temperature we observed a remarkable difference in the profile of the infrared bands, as it is possible to see in Fig.2 B. This difference is due to the structural change of the sample. The main vibrational features appear sharper and narrower if compared to those observed in Fig. 2 A. As an example, the C=O stretching mode band centred at about 1690 $cm^{-1}$ shows a FWHM of about 64 $cm^{-1}$ at 17 K, while it decreases to about 25 $cm^{-1}$ at 170 K. Other remarkable differences are the appearance of at least four components in the feature centred between 3040 and 3460 $cm^{-1}$, the sharpening and increasing intensity of the C-H stretching mode band centred at 2884 $cm^{-1}$ and the higher intensity of the C-N stretching mode band at 1328 $cm^{-1}$. These band changes are attributed to a transition between a disordered phase to a much ordered one, i.e., an amorphous to crystalline transition. A similar behaviour has been reported for many molecules, and some examples are reported by Hudgins *et al.*[36], Palumbo *et al.*[37], Modica and Palumbo[38], Moore *et al.*[39] and Abdulgalil *et al.*[40].

After the sample structural change, the acquired spectra did not show remarkable differences at higher temperatures and formamide started to sublimate from the substrate at about 220 K.

### 3.2 Formamide in water

In Fig.2 C and D we show the spectra of a mixture $NH_2CHO$:$H_2O$=1:14 deposited at 17 K and warmed up to 170 K, respectively. It should be noticed that some characteristic vibrational modes bands attributed to water overlap with those due to formamide, as in the case of the O-H stretching mode and the $NH_2$ stretching mode bands at about 3300 $cm^{-1}$, the bending mode of water and the C=O stretching mode bands at about 1660 $cm^{-1}$, and finally the libration mode of water centred at about 770 $cm^{-1}$ and the $NH_2$ wagging and torsion modes bands.

The spectrum gives useful information about the structure of the sample. In particular, the O-H dangling bonds feature centred at 3696 $cm^{-1}$ present in the spectrum acquired at 17 K (see the inset in Fig.2 C) points out that the sample is a porous amorphous film. Two different components are distinguishable, one centred at 3694 $cm^{-1}$ and one at 3716 $cm^{-1}$ attributed to three- and two-coordinate water molecules, respectively[41]. These features are not present in the spectrum acquired at 140 K because of the compaction and the crystallization of the sample[42].

In our experimental conditions pure water sublimates at about 160 K, but in this experiment its vibrational features were still visible in the spectrum we acquired at 170 K (Fig.2 panel D), even if with lower intensity. An explanation is that a fraction of the deposited water molecules interact via H-bonds with formamide, that is the major component of the sample at this temperature. As a result, an higher temperature is required to complete the water sublimation, that occurs at 180 K. Excluding the vibrational features of water, the spectrum in Fig.3 D is superimposable to the one of pure crystalline formamide at 170 K shown in the same figure (panel B). Finally, the experiment has been completed with the desorption of formamide at about 220 K.

### 3.3 Formamide in a CO matrix

In Fig.2 E we show the spectrum of a mixture $NH_2CHO$:CO=1:40 deposited at 17 K. Here the attribution of the vibrational bands is not straightforward as in the cases we have shown previously. The same spectrum is better shown in Fig.3, where most of the vibrational bands have been assigned. The spectrum include also the frequency range where the vibrations due to carbon monoxide and its isotopologues are found. For more details about CO infrared vibration modes see Baratta and Palumbo[43] and Urso *et al.*[34]. In our sample, formamide is highly diluted in carbon monoxide. The narrow vibrational bands that appear in the spectra are due to the presence of monomers and dimers, i.e., one isolated molecule or two molecules of formamide interacting with each other, respectively, and surrounded by CO molecules. This effect has been observed also for other mixtures[44]. The labels in the figure have been attributed following the works by Räsänen[45,46], Torrie and Brown[47], Lundell *et al.*[48], Mardyukov *et al.*[49] and Sivaraman *et al.*[50]. The vibrational bands assigned to water monomers and dimers (between 3600 and 3700 $cm^{-1}$ and at about 1600 $cm^{-1}$) and $CO_2$ (at 2347 $cm^{-1}$) are due to contaminants.

In our experimental conditions, pure carbon monoxide desorbs at about 32 K. In the warm up experiment of the $NH_2CHO$:CO=1:40 mixture, the 2140 $cm^{-1}$ CO stretching mode band completely disappeared at a temperature higher than 100 K, because some CO remains trapped inside the layer of formamide that is left on the substrate. At higher temperature only formamide remains, as shown in the spectrum acquired at 170 K (Fig. 2 F). Within experimental uncertainties, this spectrum is identical to the one shown in the panel B of the same figure.

### 3.4 Irradiation of a $N_2$:$CH_4$:$H_2O$=1:1:1 mixture

Kaňuchová *et al.*[29] reported that the irradiation of a frozen mixture containing nitrogen, methane, and water with 30 keV $He^+$ drives to the formation of formamide. To extend the previous work, here we show the results obtained after the irradiation

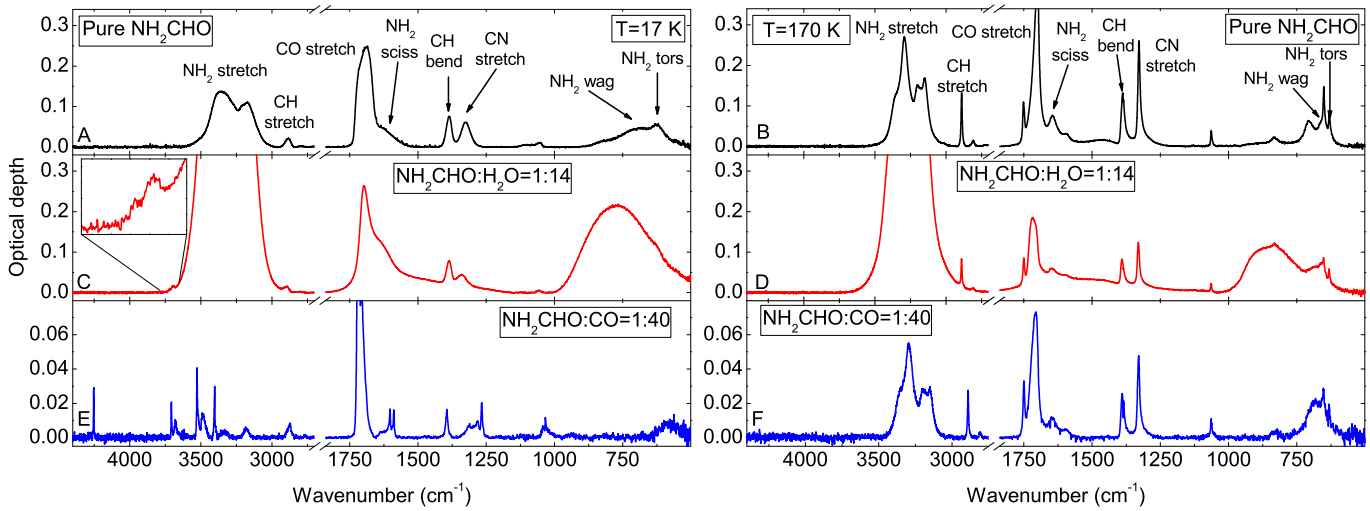


**Fig. 2** Infrared spectra in optical depth scale of pure formamide (black line, A and B) and formamide in mixture with water (red line, C and D) and carbon monoxide (blue line, E and F) acquired at 17 K (left panel) and at 170 K (right panel).

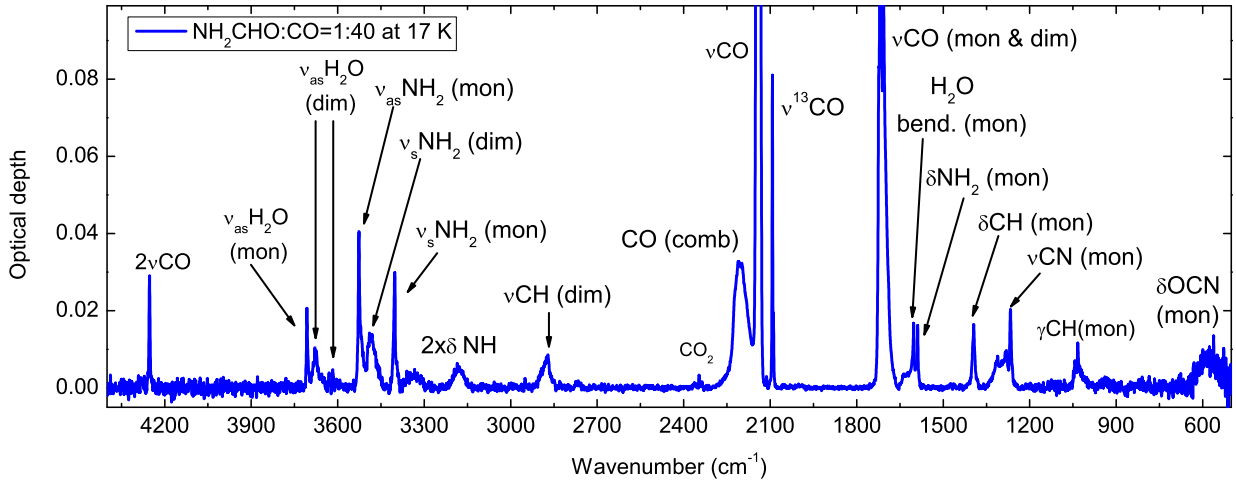


**Fig. 3** Infrared spectrum in optical depth scale of a $NH_2CHO$:CO=1:40 mixture. Labels indicate the known vibrational bands attributed to formamide, carbon monoxide and contaminants water and carbon dioxide. (mon): monomers; (dim): dimers.

of the same mixture with 200 keV $H^+$ up to a final dose of 122 eV/16u and its warm up to determine the desorption temperature of the newly synthesised formamide.

In Fig. 4 we show a comparison between the infrared spectra of pure formamide (panel A), formamide in mixture with water (panel B) and the $N_2$:$CH_4$:$H_2O$ mixture (panel C) as deposited (magenta dashed line) and after the $H^+$ bombardment (green line) at 17 K. The spectrum acquired after the irradiation exhibits not only the vibrational bands related to the deposited species, but also those due to the presence of newly formed molecules. The chemistry induced by ion bombardment is well studied for various mixtures, and it is due to the ion energy that is released along the ion track in the sample. As a consequence, molecular bonds are broken and the produced radicals and molecular fragments recombine to form new species[51–53]. The spectrum can be easly compared also to those reported by Palumbo *et al.*[54] for the same mixture after irradiation with 30 keV $He^+$ ions. Several bands fall at frequencies that have been associated to the vibrational modes of formamide by Dawley *et al.*[30] (see Table 1 in their paper). The band positions are pointed out by dashed vertical lines in Fig. 5. The spectrum acquired at the end of the irradiation (a) is compared to those acquired during the subsequent warm up of the sample. Because of the heating, volatile species leave the substrate determining the changes observed in the spectra during the experiment. On the other hand, non-volatile species remain on the substrate as a refractory residue[54–56].

As discussed in the previous sections, formamide desorbs at about 220 K, so its contribution should not appear in the infrared spectra acquired at higher temperature. However, the bands we used for its identification are still present in our sample even in the spectrum acquired after we kept the sample under vacuum at 296 K for 24 hours.

## 4 Discussion

According to our experimental results, pure formamide crystallize at 170 K and desorbs from the substrate at about 220 K. We have not observed remarkable differences in the crystallization temperature of formamide when in mixture with water, the latter sublimating at 180 K and leaving pure crystalline formamide on the substrate up to about 220 K. When formamide has been diluted in CO, its infrared spectral features allowed us to determine the presence of monomers and dimers in the sample. CO started to desorb at about 40 K, and completely left the sample at a temperature higher than 100 K. Because of the high dilution of formamide, we expected that during the sublimation of CO, it could drag also formamide into the gas phase. However, we observed that formamide remained on the substrate up to 220 K. Other examples concerning molecules diluted in a volatile matrix which do not desorb when the matrix sublimates have been reported in literature. Brucato *et al.*[57] showed that carbonic acid

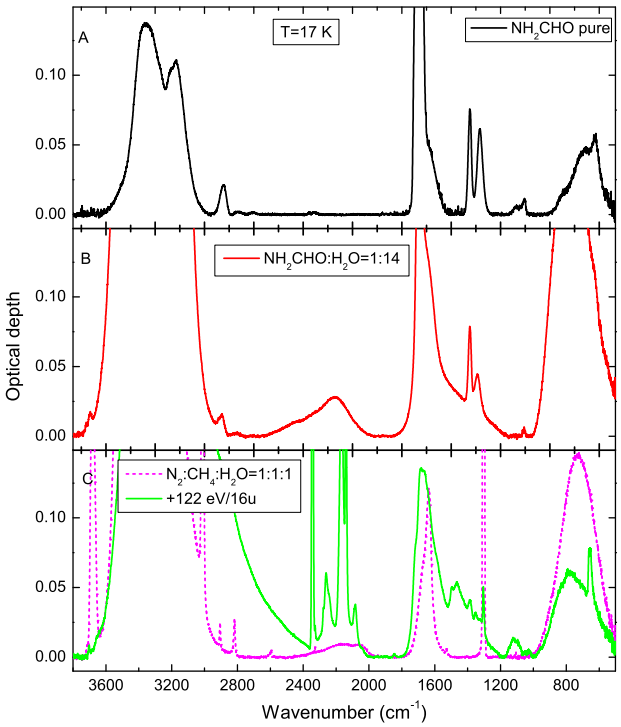


**Fig. 4** Comparison between spectra acquired at 17 K for pure formamide (panel A), formamide in water (panel B) and a mixture containing nitrogen, water and methane (panel C) as deposited (magenta dashed line) and after irradiation with 200 keV $H^+$ up to 122 eV/16 u (green line).

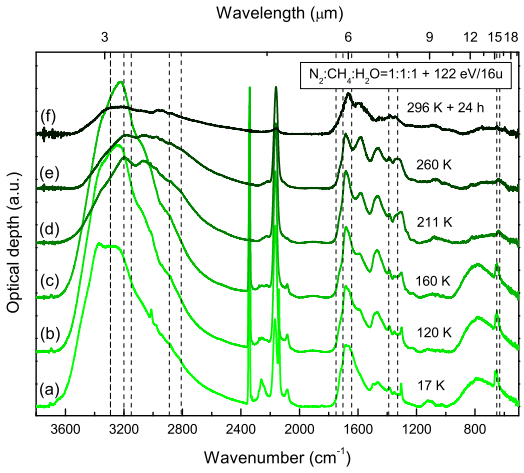


**Fig. 5** IR spectra of a $N_2$:$CH_4$:$H_2O$=1:1:1 mixture irradiated with 200 keV $H^+$ at 17 K up to 122 eV/16u and warmed up to 296 K. All the spectra are shown in optical depth scale and displaced by an arbitrary offset for clarity. Vertical dashed lines represent the vibrational frequencies of pure formamide at 165 K as reported by Dawley *et al.*[30]

is produced after the irradiation of mixtures containing water and carbon dioxide with 1.5-3 keV H or He ions. Carbonic acid remains on the substrate as a residual film up to 247 K, while volatile species sublimate at lower temperatures. Burke *et al.*[58] reported about experiments in which methyl formate, acetic acid and glycoladehyde were mixed or adsorbed on water ice at 20 K and warmed up until the complete sublimation of the sample. In their Time Programmed Desorption (TPD) experiments, they observed that methyl formate desorbs at about 145 K, when it is released by the pores in the water ice and glycolaldehyde co-desorbs with water at about 160 K. For the acetic acid:water mixture they observed that the acid can remain on the substrate up to about 175 K, after water desorption.

The irradiation of the $N_2$:$CH_4$:$H_2O$ mixture with 200 keV $H^+$ allowed us to detect formamide among the synthesised molecules in the sample, confirming the results reported by Kaňuchová *et al.*[29]. During the warm up of the sample, after the volatiles sublimation, the formamide vibrational features were detectable up to 296 K in the residue that has been formed on the substrate. This result strongly suggests that once formamide is formed because energetic processing, it remains trapped inside the refractory organic residue.

It is possible to notice a remarkable difference in the desorption temperature of formamide as pure or in mixtures we reported if compared to the experiments reported by Dawley *et al.*[30]. In their experiments the complete desorption requires about 380 K. In our opinion, the higher temperature required for the formamide desorption is due to the porous substrate they used to simulate the dust grains, so that molecules penetrates it during the deposition, remaining trapped through the warm up. In our experiments the deposition is limited on the KBr substrate surface, allowing the desorption at a lower temperature. However, the irradiation experiment and the subsequent heating of the sample have shown that formamide remains trapped in the refractory residue. This effect can be somehow compared to the trapping observed by Dawley *et al.*[30] into the porous substrate. Even if the chemical and physical properties of these materials are completely different, both slow down the sublimation because they act as physical barriers, requiring an higher temperature to allow the desorption.

These results can be applied in an astrophysical context. As already said, formamide has been detected in the gas phase in the line of sight to star forming regions and tentatively identified in the solid phase in ISO-SWS infrared spectra of proto-stars, as reported by Schutte *et al.*[19] and Raunier *et al.*[20]. Calculations have suggested that it can be formed directly in the gas phase[24,25]. Also, energetic processing experiments have shown that its formation is efficient on the icy mantles of dust grains and can explain the observed gas phase abundances if a desorption mechanism is taken into account. The sublimation temperature we determined in laboratory experiments for formamide when pure and in mixture is about 220 K. In the case of its formation after energetic processing of icy mantles analogues, because of its trapping in the residue, the temperature required is higher than 296 K.

It is interesting to couple these data with the work reported by López-Sepulcre *et al.*[7]. By means of the 30 m IRAM radio telescope they searched for formamide rotational lines toward several star forming regions within the large program Astrochemical Surveys At IRAM (ASAI). Among them, in proto-stellar objects IRAS 4A, SVS13A, OMC-2 FOR 4, Cep E and I16293 they have been able to detect formamide and to estimate its column density. For what concern colder sources, i.e., L1544, TMC1, B1, L1527 and L1157-mm, they have detected no formamide. These results suggest that temperatures of a few tens K would determine the non desorption or a very slow desorption of formamide, explaining its absence in the gas-phase of dark cold clouds, while in hotter sources like pre- and proto-stellar clouds, where the temperature can be higher than 100 K, the sublimation takes place in the time scale of stellar formation, so that it is possible to detect its rotational lines. Also, other desorption mechanism have to be taken into account if temperature is not high enough to explain formamide sublimation. As an example, cosmic-ray ion erosion of volatiles from dust grains[59] and mantles explosion due to impulsive spot heating on grains[60] could drag formamide into the gas-phase together with other solid phase molecules.

Formamide has been found in the coma of comet C/1995 O1 Hale-Bopp[22], comet C/2012 F6 Lemmon and comet C/2013 R1 Lovejoy[23]. These detections are interesting because comets are the result of grains accretion, and our experimental data strengthen the hypothesis that formamide is there since the early stage of the Solar System formation, when these objects have been formed. Also, the exposure to radioactive element decay and cosmic rays may have contributed to increase its abundance. More recently, new results have been obtained by the European Space Agency Rosetta mission. Rosetta orbited the comet 67P/Churyumov-Gerasimenko and sent the lander Phylae on its surface. Both the orbiter and the lander were equipped with several instruments that allowed to investigate the physical and chemical properties of the comet and its coma. le Roy *et al.*[61] reported an inventory of the volatile species detected by the Double Focusing Mass Spectrometer (DFMS) of the ROSINA experiment on board of Rosetta. Among the detected molecules, they have been able to establish only upper limits for the presence of formamide, found to be $<1\times10^{-4}$ and $<1\times10^{-3}$ w.r.t. water (in %) in the summer and in the winter hemisphere, respectively. On the other hand, Goesmann *et al.*[62] used formamide, among the other molecules, to fit the Cometary Sampling and Composition (COSAC) mass spectrum obtained by the Philae lander on the comet surface. They reported that the abundance of this molecule can be as high as 1.8% w.r.t. water. It is generally accepted that the dark refractory surface of a comet, i.e., the crust, is formed

after cosmic-ray bombardment[32]. Taking into account our data, we suggest that the missing detection of formamide in the coma of comet 67P/Churyumov-Gerasimenko[61] and its simultaneous presence on the surface[62] is due to the fact that formamide is trapped in the crust of the comet because the temperature experienced throughout its orbit was not high enough to determine its sublimation.

To strengthen this work, the detection of solid-state formamide in star forming regions would be of great importance. By this point of view, we expect that interesting results will be collected by the Near Infrared Spectrograph (NIRSpec) and the Mid-Infrared Instrument (MIRI) on board the James Webb Space Telescope (JWST), which launch is expected to be in October 2018.

## 5 Acknowledgements

This work has been supported by the Italian Ministero dell'Istruzione, dell'Università e della Ricerca through the grant Progetti Premiali 2012-iALMA (CUP C52I13000140001). Zuzana Kaňuchová was supported by VEGA - The Slovak Agency for Science, Grant No. 2/0032/14. This work has been also supported by COST Action TD1308 - ORIGINS.

## References

1 R. Saladino, C. Crestini, V. Neri, J. R. Brucato, L. Colangeli, F. Ciciriello, E. di Mauro and G. Costanzo, *ChemBioChem*, 2005, **6**, 1368–1374.

2 R. Saladino, C. Crestini, F. Ciciriello, S. Pino, G. Costanzo and E. di Mauro, *Research in Microbiology*, 2009, **160**, 441–448.

3 R. Saladino, C. Crestini, S. Pino, G. Costanzo and E. di Mauro, *Physics of Life Reviews*, 2012, **9**, 84–104.

4 S. Pino, J. E. Sponer, G. Costanzo, R. Saladino and E. di Mauro, *Life*, 2015, **5**, 372–384.

5 R. H. Rubin, G. W. S. Tr., R. C. Benson, H. L. Tigelaar and W. H. Flygare, *ApJ*, 1971, **169**, L39–L44.

6 E. Mendoza, B. Lefloch, A. López-Sepulcre, C. Ceccarelli, C. Codella, H. Boechat-Roberty and R. Bachiller, *MNRAS*, 2014, **445**, 151–161.

7 A. López-Sepulcre, A. A. Jaber, E. Mendoza, B. Lefloch, C. Ceccarelli, C. Vastel, R. Bachiller, J. Cernicharo, C. Codella, C. Kahane, M. Kama and M. Tafalla, *MNRAS*, 2015, **449**, 2438–2458.

8 J. M. Greenberg, *Molecules in the Galactic Environment*, Wiley, New York, M. A. Gordon and L. E. Snyder edn, 1973.

9 H. Rothard, A. Domaracka, P. Boduch, M. E. Palumbo, G. Strazzulla, E. F. de Silveira and E. Dartois, *Journal of Physics B*, 2017, **50**, 062011.

10 E. Dartois and L. d'Hendecourt, *A&A*, 2001, **365**, 144–156.

11 E. Dartois, W. F. Thi, T. R. Geballe, D. Deboffle, L. d'Hendecourt and E. van Dischoeck, *A&A*, 2003, **399**, 1009–1020.

12 A. C. A. Boogert, W. A. Schutte, F. P. Helmich, A. G. G. M. Tielens and D. H. Wooden, *A&A*, 1997, **317**, 929–941.

13 E. L. Gibb, D. C. B. Whittet, A. C. A. Boogert and A. G. G. M. Tielens, *ApJSS*, 2004, **151**, 35–73.

14 E. Dartois, *Space Sci Rev*, 2005, **119**, 293–310.

15 K. I. Öberg, A. C. A. Boogert, K. M. Pontoppidan, S. van den Broek, E. F. van Dishoeck, S. Bottinelli, G. A. Blake and N. J. Evans, *ApJ*, 2011, **740**, 109.

16 A. C. A. Boogert, P. A. Gerakines and D. C. B. Whittet, *ARA&A*, 2015, **53**, 541–581.

17 W. A. Schutte, P. A. Gerakines, E. F. van Dishoeck, J. M. Greenbergand and T. R. Geballe, *AIP Conference Proceedings*, 1994, **312**, 73.

18 M. E. Palumbo, T. R. Geballe and A. G. G. M. Tielens, *ApJ*, 1997, **479**, 839–844.

19 W. A. Schutte, A. C. A. Boogert, A. G. G. M. Tielens, D. C. B. Whittet, P. A. Gerakines, J. E. Chiar, P. Ehrenfreund, J. M. G. E. F. van Dishoeck and T. de Graauw, *A&A*, 1999, **343**, 966–976.

20 S. Raunier, T. Chiavassa, F. Duvernay, F. Borget, J. P. Aycard, E. Dartois and L. d'Hendecourt, *A&A*, 2004, **416**, 165–169.

21 P. Caselli and C. Ceccarelli, *A&AR*, 2012, **20**, 56.

22 D. Bockelè-Morvan, D. C. Lis, J. E. Wink, D. Despois, J. Crovisier, R. Bachiller, D. J. Benford, N. Biver, P. Colom, J. K. Davies, E. Gèrard, B. Germain, M. Houde, D. Mehringer, R. Moreno, G. Paubert, T. G. Phillips and H. Rauer, *A&A*, 2000, **353**, 1101–1114.

23 N. Biver, D. Bockelèe-Morvan, V. Debout, J. Crovisier, J. Boissier, D. C. Lis, N. dello Russo, R. Moreno, P. Colom, G. Paubert, R. Vervack and H. A. Weaver, *A&A*, 2014, L5.

24 V. Barone, C. Latouche, D. Skouteris, F. Vazart, N. Balucani, C. Ceccarelli and B. Lefloch, *MNRAS*, 2015, **453**, L31–L35.

25 F. Vazart, D. Calderini, C. Puzzarini and D. S. V. Barone, *JCTC*, 2016, **12**, 5385–5397.

26 P. A. Gerakines, M. H. Moore and R. L. Hudson, *Icarus*, 2004, **170**, 202–213.

27 B. M. Jones, C. Bennett and R. I. Kaiser, *ApJ*, 2011, **734**, 78.

28 B. L. Henderson and M. S. Gudipati, *ApJ*, 2015, **800**, 66–83.

29 Z. Kaňuchová, R. G. Urso, G. A. Baratta, J. R. Brucato, M. E. Palumbo and G. Strazzulla, *A&A*, 2016, **585**, A155.

30 M. M. Dawley, C. Pirim and T. M. Orlando, *J. Phys. Chem. A*, 2014, **118**, 1220–1227.

31 J. F. Ziegler, J. P. Biersack and M. D. Ziegler, *The Stopping and Range of Ions in Solids*, Pergamon Press, New York, 2008.

32 G. Strazzulla and R. E. Johnson, *Irradiation Effects on Comets and Cometary Debris, Comets in the post-Halley era*, Springer Netherlands, Dordrecht, 1991.

33 D. Fulvio, B. Sivaraman, G. A. Baratta, M. E. Palumbo and N. J. Mason, *Spectrochimica Acta A Molecula and Biomolecular Spectroscopy*, 2009, **72**, 1007–1013.

34 R. G. Urso, C. Scirè, G. A. Baratta, G. Compagnini and M. E. Palumbo, *A&A*, 2016, **594**, A80.

35 M. E. Palumbo, G. A. Baratta, M. P. Collings and M. R. S. McCoustra, *PCCP*, 2006, **8**, 279–284.

36 D. M. Hudgins, S. A. Sandford, L. J. Allamandola and A. G. G. M. Tielens, *AjPS*, 1993, **86**, 713–870.

37 M. E. Palumbo, A. C. Castorina and G. Strazzulla, *A&A*, 1999, **342**, 551–562.

38 P. Modica and M. E. Palumbo, *A&A*, 2010, **519**, A22.

39 M. H. Moore, R. F. Ferrante, W. J. Moore and R. Hudson, *ApJS*, 2010, **191**, 96–112.

40 A. G. M. Abdulgalil, D. Marchione, J. D. Thrower, M. P. Collings, M. R. S. McCoustra, F. Islam, M. E. Palumbo, E. Congiu and F. Dulieu, *Phil Trans R Soc A*, 2013, **371**,.

41 M. E. Palumbo, *A&A*, 2006, **453**, 903–909.

42 J. B. Bossa, K. Isokoski, M. S. de Valois and H. Linnartz, *A&A*, 2012, **545**, A82.

43 G. A. Baratta and M. E. Palumbo, *J. Opt. Soc. Am. A*, 1998, **15**, 3076–3085.

44 P. Ehrenfreund, P. A. Gerakines, W. A. Schutte, M. C. van Hemert and E. F. van Dishoeck, *A&A*, 1996, **312**, 263–274.

45 M. Räsänen, *Journal of Mol. Structure*, 1983a, **101**, 275–286.

46 M. Räsänen, *Journal of Mol. Structure*, 1983b, **102**, 235–242.

47 B. H. Torrie and B. A. Brown, *J. Raman Spectroscopy*, 1994, **25**, 183.

48 J. Lundell, M. Krajewska and M. Räsänen, *J. Phys. Chem. A*, 1998, **102**, 6643–6650.

49 A. Mardyukov, E. Sánchez-Garcia, P. Rodziewicz, N. L. Doltsinis and W. Sander, *J. Phys. Chem. A*, 2007, **111**, 10552–10561.

50 B. Sivaraman, B. N. R. Sekar, B. G. Nair, V. Hatode and N. J. Mason, *Spectrochimica Acta A*, 2013, **105**, 238–244.

51 A. Trottier and R. Brooks, *ApJ*, 2004, **612**, 1214–1221.

52 E. Seperuelo-Duarte, A. Domaracka, P. Boduch, H. Rothard, E. Dartois and E. F. de Silveira, *A&A*, 2010, **512**, A71.

53 F. Islam, G. A. Baratta and M. E. Palumbo, *A&A*, 2014, **A73**,.

54 M. E. Palumbo, G. Ferini and G. A. Baratta, *Advances in Space Research*, 2004, **33**, 49–556.

55 G. Ferini, G. A. Baratta and M. E. Palumbo, *A&A*, 2004, **4**, 757–766.

56 G. A. Baratta, D. Chaput, H. Cottin, L. F. Cascales, M. E. Palumbo and G. Strazzulla, *Planetary and Space Science*, 2015, 211–220.

57 J. R. Brucato, M. E. Palumbo and G. Strazzulla, *Icarus*, 1997, **125**, 135–144.

58 D. J. Burke, F. Puletti, P. M. Woods, S. Viti, B. Slater and W. A. Brown, *The Journal of Chemical Physics*, 2015, **143**, 164704–16.

59 E. M. Bringa and R. E. Johnson, *ApJ*, 2004, **603**, 159–164.

60 A. V. Ivlev, T. B. Röcker, A. Vasyunin and P. Caselli, *ApJ*, 2015, **805**, 59.

61 L. le Roy, K. Altwegg, H. Balsiger, J. J. Berthelier, A. Bieler, C. Briois, U. Calmonte, M. R. Combi, J. D. Keyser, F. Dhooghe, B. Fiethe, S. A. Fuselier, S. Gasc, T. I. Gombosi, M. Hässig, A. Jäckel, M. Rubin and C. Y. Tzou, *A&A*, 2015, **583**, A2.

62 F. Goesmann, H. Rosenbauer, J. H. Bredehöft, M. Cabane, P. Ehrenfreund, T. Gautier, C. Giri, H. Krüger, L. le Roy, A. J. MacDermott, S. McKenna-Lawlor, U. J. Meierhenrich, G. Munoz-Caro, F. Raulin, R. Roll, A. Steele, H. Steininger, R. Sternberg, C. Szopa, W. Thiemann and S. Ulamec, *Science*, 2015, **349**, aab06891–3.